P2 - Building Built In Minutes: SfM and NeRF

Mihir Deshmukh
Robotics Engineering
Worcester Polytechnic Institute
Email: mpdeshmukh@wpi.edu

Ashwin Disa
Robotics Engineering
Worcester Polytechnic Institute
Email: amdisa@wpi.edu

***Abstract*—In this project assignment, we reconstruct a 3D scene and simultaneously obtain the camera poses of a monocular camera with respect to the given scene also known as Structure from Motion. We create the rigid structure from a set of images with different view points. For the second phase we implement the famous NeRF (Reural Radiance Fields) for synthesizing novel views of complex scenes by optimizing an underlying continuous volumetric scene function using a sparse set of input views.**

I. Phase 1: Structure from Motion

A. Dataset

We are given with a set of 5 images of Unity Hall at WPI as shown in fig. 1, using a Samsung S22 Ultra's primary camera at f/1.8 aperture, ISO 50 and 1/500 sec shutter speed. The camera is calibrated after resizing using a Radial-Tangential model with 2 radial parameters and one tangential parameter using the MATLAB R2022a's Camera Calibrator Application beforehand. The images provided are already distortion-corrected and resized to $800 \times 600px$.

Fig. 1. Dataset.

B. Feature Matching, estimating fundamental matrix and RANSAC

We are also given matched features. We reject the outliers from the same set using RANSAC. We do so using an estimation of the fundamental matrix, which is based on the epipolar constraint given by $x_i^T F x_i = 0$. F is 3×3 matrix, which we get by solving a homogeneous linear system $Ax = 0$ with nine unknowns applying the Singular Value Decomposition (SVD). We do so by taking eight random points from the pool of matches and estimating a rough F matrix, computing the epipolar constraint, and comparing it with a threshold value. We then estimate the final F matrix using the inliers from RANSAC. We utilize the inliers from cv2 for a more robust result but our Ransac inliers implementation also works effectively. Due to noise in the matches, the estimated F matrix can be of rank three i.e. $\sigma_9 \neq 0$. So, to enforce the rank two constraint, the last singular value of the estimated F is set to zero. This also results in all the epipolar lines intersecting at a single point known as the epipole. The epipolar lines for a pair of images are shown in Fig. 2. The epipole is the other camera position in the first image frame; hence, the point is not visible in the image.

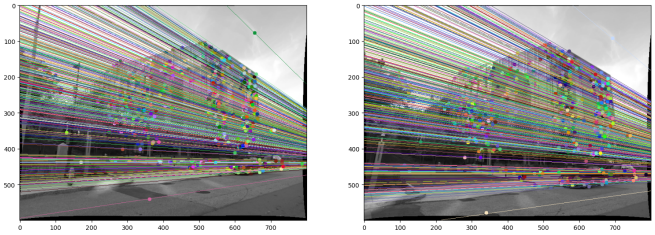

Fig. 2. Epipolar lines for a pair of images.

The final F matrix we got is shown below:

$$F_{final} = \begin{bmatrix} -1.607e-07 & -3.011e-05 & 1.343e-02 \\ 3.266e-05 & 3.202e-06 & -3.486e-02 \\ -1.518e-02 & 3.304e-02 & 1.000e+00 \end{bmatrix}$$

C. Estimate Essential Matrix from Fundamental Matrix

The essential matrix is another 3×3 matrix, but with some additional properties that relate the corresponding points, assuming that the cameras obey the pinhole model. The matrix is given by $E = K^T F K$, where K is the camera intrinsic matrix. E is reconstructed with $(1, 1, 0)$ singular values due to the noise in K given by $E = USV^T$, where S is a diagonal matrix with the given singular values. The estimated Essential matrix is given by:

$$E_{final} = \begin{bmatrix} -9.666e-05 & -5.827e-01 & 1.395e-01 \\ 6.355e-01 & 5.369e-02 & -7.511e-01 \\ -1.880e-01 & 7.960e-01 & 2.791e-02 \end{bmatrix}$$

D. Estimate Camera Pose from Essential Matrix

The camera pose consists of 6 DOF, Rotation (Roll, Pitch, Yaw), and Translation (X, Y, Z) of the camera with respect to the world. The camera pose is estimated from $P = KR[I_{3\times3} - C]$. These four pose configurations can be computed from E matrix where $E = UDV^T$, and $W = \begin{bmatrix} 0 & -1 & 0 \\ 1 & 0 & 0 \\ 0 & 0 & 1 \end{bmatrix}$. The four configurations are $C_1 = U(:, 3)$ and $R_1 = UWV^T$, $C_2 = -U(:, 3)$ and $R_2 = UWV^T$, $C_3 = U(:, 3)$ and $R_3 = UW^TV^T$, $C_4 = -U(:, 3)$ and $R_4 = UW^TV^T$. Also if

$det(R) = -1$, the camera pose is corrected i.e $C = -C$ and $R = -R$.

E. Triangulation Check for Cheirality Condition

We found four camera poses by decomposing the Essential matrix. Only one of them is accurate. We triangulate the 3D points given any two camera poses and the matched features and plot all the 3D points as shown in 3. We disambiguate the camera poses by checking the cheirality constraint, which determines if the point is behind the camera. We triangulate the 3D points using linear least squares to check the sign of the depth Z in the camera coordinate system w.r.t. camera center. A 3D point X is in front of the camera $r_3(X - C) > 0$ where r_3 is the third row of the rotation matrix (z-axis of the camera). The pose with the most number of points satisfying the constraint is the true camera pose. Now that we have the camera pose configurations and their linear triangulated points.

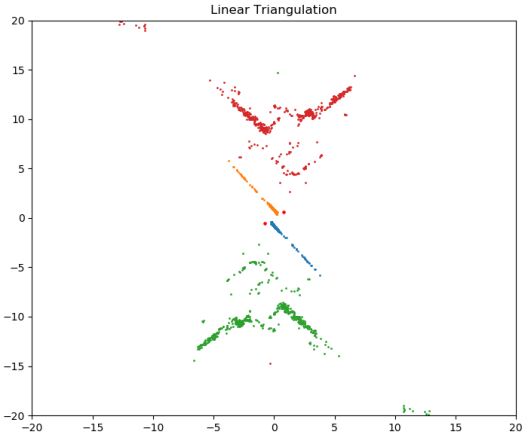

Fig. 3. Triangulated 3D points from 2 camera poses.

To better estimate the triangulated points, we solve a nonlinear minimization problem. The located triangulated points, X, are considered as the initial guess for the problem where we try to minimize the reprojection error. We solve using nonlinear optimization function $scipy.optimize.least\_squares()$. The results are compared with the linear triangulation, which is shown in Fig. 4.

F. Perspective-n-points

With the world points from nonlinear triangulation, intrinsic parameters, and common points, the camera poses are estimated using LinearPnP. Here, we again get a linear equation and solve it using SVD to get the projection matrix. The rotation and camera poses are extracted from the same matrix. The estimation may not be accurate due to underlying outliers that were removed using PnPRANSAC. The reprojection error is minimized using nonlinear PnP using least squares. The camera poses and all world points are shown in Fig. 7.

The reprojection errors are listed in the following table.

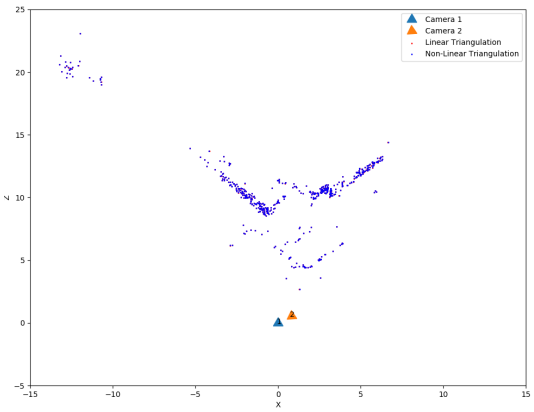

Fig. 4. Linear and nonlinear triangulated 3D points from 2 camera poses.

Fig. 5. Reprojected points after linear triangulation.

Error	
Linear reprojection	6.8731
Nonlinear reprojection	6.840
Linear PnP (1,3)	777.91
Nonlinear PnP (1,3)	726.17
Linear PnP (1,4)	19.44
Nonlinear PnP (1,4)	7.486
Linear PnP (1,5)	44.71
Nonlinear PnP (1,5)	3.613

G. Visibility matrix and bundle adjustment

We create a visibility matrix for the given number of cameras and total world points. The function initializes the matrix with zeros and iterates over each world point and camera to mark the visibility of the world point in each camera. Fig. 8 shows the Visibility matrix size and how each column shows if a world point is visible in each of the camera view. Next, we use bundle adjustment to reduce the projection error simultaneously for all the 5 images using this visibility matrix. Bundle adjustment takes input parameters related to camera poses, 3D points, visibility, and intrinsic matrix and uses least squares optimization to refine the camera poses and 3D points. The function returns the optimized camera

Fig. 6. Reprojected points after nonlinear triangulation.

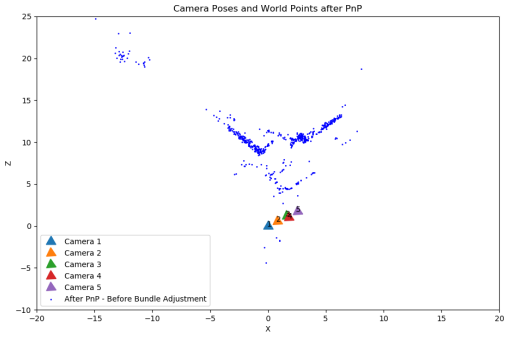

Fig. 7. Camera poses after nonlinear PnP.

poses and 3D points. This is shown in 9, which shows bundle adjustment for all the camera views.

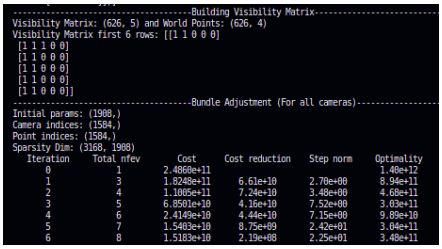

```
-----------------------------------Building Visibility Matrix-----------------------------------
Visibility Matrix: (626, 5) and World Points: (626, 4)
Visibility Matrix first 6 rows: [[1 1 0 0 0]
 [1 1 1 0 0]
 [1 1 0 0 0]
 [1 1 0 0 0]
 [1 1 0 0 0]
 [1 1 0 0 0]]
-----------------------------------Bundle Adjustment (For all cameras)-----------------------------------
Initial params: (1908,)
Camera indices: (1584,)
Point indices: (1584,)
Sparsity Dim: (3168, 1908)
   Iteration     Total nfev        Cost      Cost reduction    Step norm     Optimality
       0              1         2.4868e+11                                    1.40e+12
       1              3         1.8248e+11      6.61e+10       2.70e+00       8.94e+11
       2              4         1.1085e+11      7.24e+10       3.48e+00       4.68e+11
       3              5         6.8501e+10      4.16e+10       7.52e+00       3.03e+11
       4              6         2.4149e+10      4.44e+10       7.15e+00       9.89e+10
       5              7         1.5403e+10      8.75e+09       2.42e+01       3.04e+11
       6              8         1.5183e+10      2.19e+08       2.25e+01       3.48e+11
```

Fig. 8. Visibility matrix size and Sample entries.

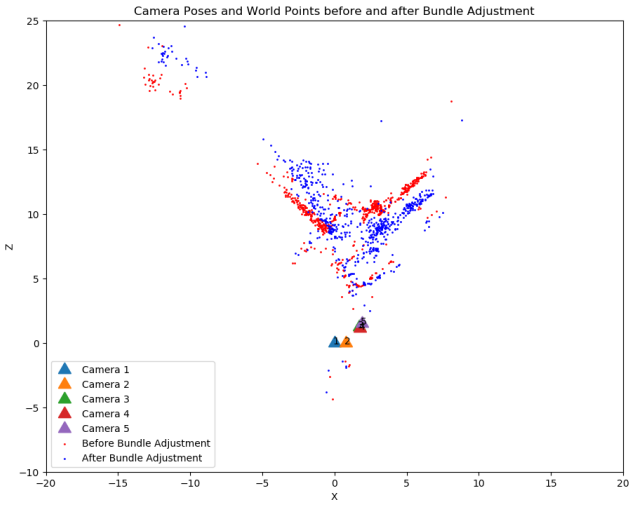

Fig. 9. Camera poses and world points after bundle adjustment.

II. Phase: 2 Deep Learning Approach

We implement the NeRF model as mentioned in the paper which is a method for representing 3D scenes by being able to synthesize novel views after optimizing the network using a sparse set of input views.

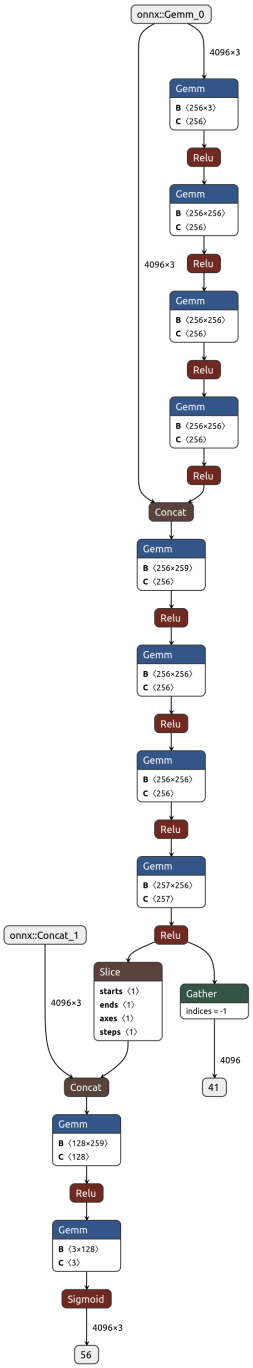

Fig. 10. Model Architecture.

A. DataSet

We use the dataset given by the original authors of the paper. A parser function reads data from a JSON file, processes the data to load images and their related information, and prepares the data for further processing. It returns information about the camera, images, poses, and camera information like focal length, and similarly for the test data.

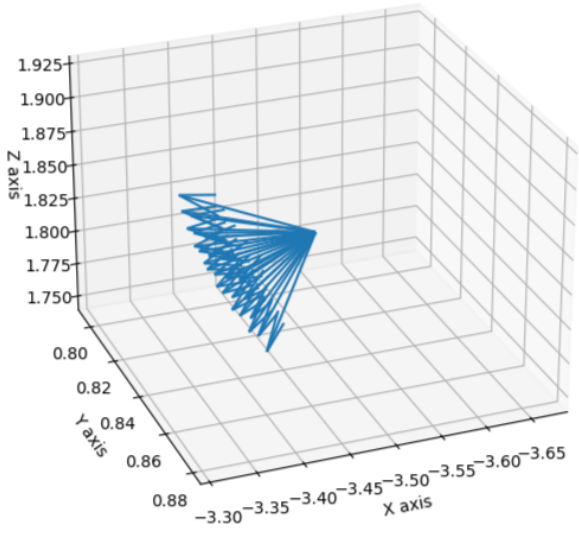

Fig. 11. Ray Directions from the origin in world frame.

B. Pixel to Ray

We use a pinhole model of a camera and with the given information such as the camera matrix and the transformation between the camera pose and world frame to estimate the ray origin and unit vector along the ray direction. NeRF requires rays from each pixel of the image. The number of rays for each image is equal to the number of pixels in the image, in our case we reduce the 800×800 image into 400×400, totaling to e number of rays for each image is equal to the number of pixels in the image, in our case we reduce the 800×800 image into 400×400, totaling 160000 rays per image. An illustration of one such set of rays from an image is shown in Fig. 11.

C. Volume Rendering

The model outputs the RGB and volume density for different samples along the rays. For each sample point along each ray, we query the NeRF model to obtain color and density values at these points and then apply volume rendering techniques to compute the final RGB image. The volume rendering process involves computing alpha values based on density and distance, which are then used to calculate weights for RGB. These weights are utilized to blend the sampled colors along the rays, resulting in the RGB map representing the rendered image.

D. Model Architecture

We adopted the same architecture as given in the paper which consists of 8 fully connected layers. We also include

a skip connection that concatenates this input to the fifth layer's activation. After the next four fully connected layers we extract the sigma output and the feature map. This feature vector is concatenated with the positional encoding of the input viewing direction $(\gamma(d))$ and is processed by an additional fully connected ReLU layer with 128 channels. A final layer (with a sigmoid activation) outputs the emitted RGB radiance at position x, as viewed by a ray with direction d. The position encoding lengths were set to 10 and 4 each for ray query points and ray directions respectively following the original implementation. The model architecture is shown in Fig. 10.

E. Training

For training, we first generate all the rays associated with all the images in the dataset. Then, 4096 (batch size) number of rays are sampled randomly from the whole dataset. This ensures rays from multiple viewpoints go in during training in one batch thus preventing the model from overfitting to one image. The training of 80000 iterations took about 6 hours to complete for each dataset with Pytorch automatic mixed precision turned on for memory efficiency.

We use the following hyperparameters for training NeRF:

- No of iterations: 80000
- Learning Rate: $5e^{-4}$
- Optimizer: Adam (Default beta values)
- T_near: 2
- T_far: 6
- Batch_size: 4096
- Number of query points per ray: 192

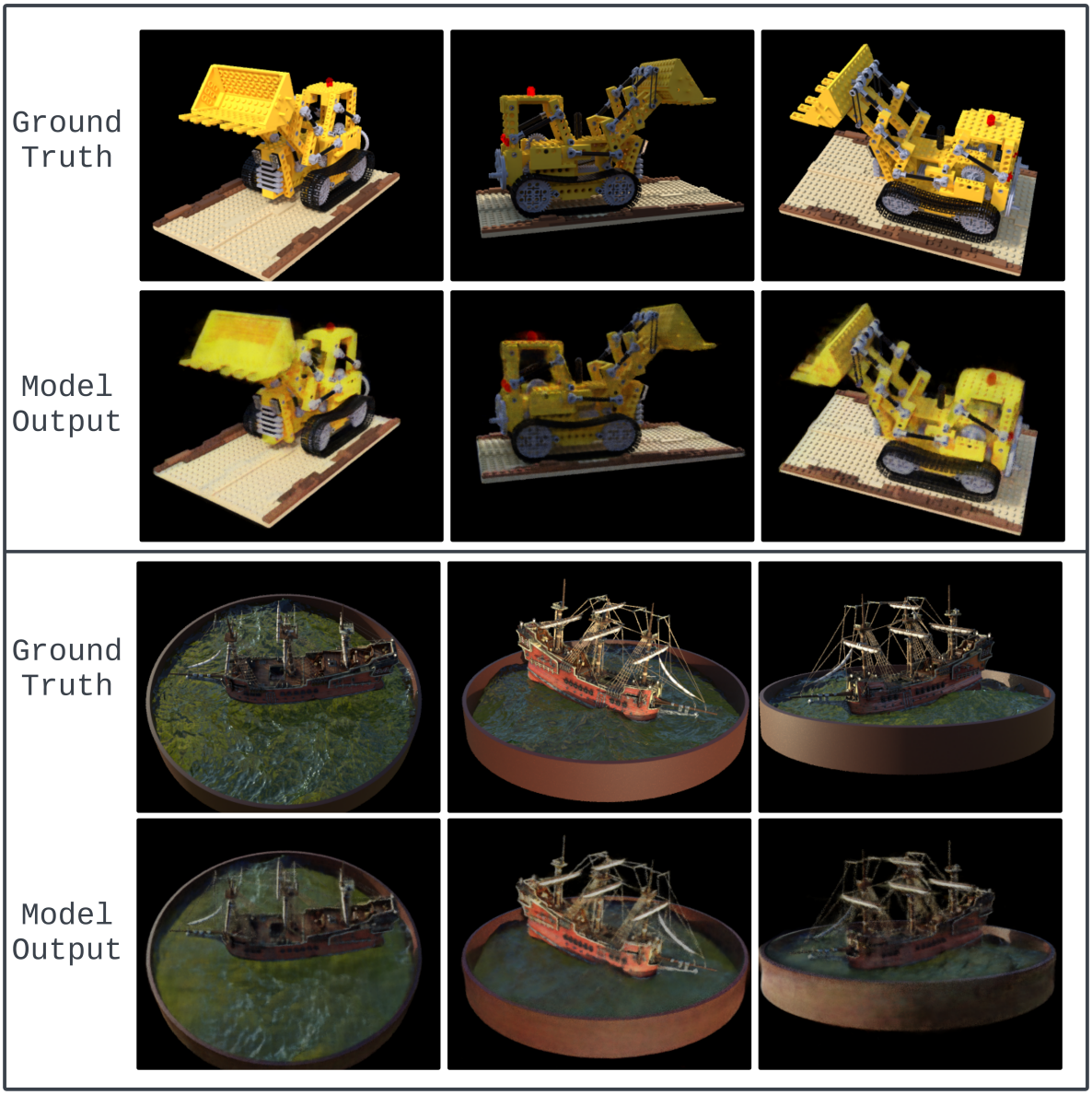

Fig. 12. Original and predicted image for Lego and Ship dataset.

F. Results

The best models were from the 53800 iterations for the Lego set and 58100 iterations for the ship dataset. Following are the PSNR and SSIM of the trained model on the test set.

1) Lego test set:
   - Average PSNR: 25.51
   - Average SSIM: 0.883
2) Ship test set:
   - Average PSNR: 26.95
   - Average SSIM: 0.832

1) Result Analysis: The results look pretty good after training as evidenced by the results shown in Fig. 12. The GIFs for both models are attached with the submission. Some novel views do perform better which have better illumination. This can be clearly seen in both models with brighter perspective outputs doing much better as we get a higher SSIM.

The finer details on the lego as well as the ship are not as clear as the original image. We also need to incorporate hierarchical sampling to get finer details as explained in the original NeRF paper. Also, training for even more number of iterations will help improve the model performance.

2) Without Position Encoding: Our model didn't converge without the positional encoding. We tried multiple lower as well as higher learning rates as well as the number of query points along the rays but the loss kept constant. The output was just a black image with no information.

III. Reference

B. Mildenhall, P. P. Srinivasan, M. Tancik, J. T. Barron, R. Ramamoorthi, and R. Ng, "NeRF: Representing Scenes as Neural Radiance Fields for View Synthesis." arXiv, 2020. doi: 10.48550/ARXIV.2003.08934.